Environ Earth Sci (2010) 59:1693–1702
DOI 10.1007/s12665-009-0151-0

ORIGINAL ARTICLE

# Landslides affecting sedimentary characteristics of reservoir basin

**Chien-Yuan Chen · Lien-Kuang Chen · Fan-Chieh Yu · Sheng-Chi Lin · Yu-Ching Lin · Chou-Lung Lee · Yu-Ting Wang**

Received: 31 August 2008 / Accepted: 16 March 2009 / Published online: 7 April 2009


**Abstract** Typhoons Aere (2004) and Matsa (2005) caused high nephelometric turbidity in the Shihmen reservoir in northern Taiwan, jeopardizing the operation of the reservoir for several days, and ultimately impacting the living conditions and economy of the downstream residents. The torrential rains caused landslides and debris flows in upland areas, and flowed into riverbeds, likely contributing significantly to the suspended sediment yields in the reservoir. This investigation elucidates how upland landslides affect sediment attributes in the reservoir basin. Study methods including field observations, spatial analysis in GIS and aerial photo interpretation are adopted to trace the sediment sources and contributing factors to the landslide. Torrential rains induced landslides and debris-flows upland, causing river incisions and soil erosion in landslide areas lacking vegetation. These factors, together with the conditions of the engineered structures and geologic vulnerabilities of the area, caused suspended sediment yield in the reservoir. The high nephelometric turbidity could potentially reoccur, with masses of landslide-derived sediment remaining upland and in the riverbed.

**Keywords** Landslide · Sediment yield · Soil erosion · Suspended sediment · Shihmen reservoir

## Introduction

The Shihmen Reservoir, which was finished in 1964, was constructed to reduce drought and promote agricultural development, because the upstream area is high and precipitous but unable to store water. Due to the rising population in downstream urban communities, the reservoir is now a multipurpose hydraulic engineering project providing irrigation, power generation, public water supply and flood control.

Typhoon Aere hit Taiwan and brought 1,600 mm of maximum total rain to the Shihmen Reservoir basin during the period 23–26 August 2004. Additionally, it caused many landslides and debris flows upland, sediment flux in the truck river, Tahan Stream, increasing the nephelometric turbidity unit (NTU), and thus jeopardized the water supply of the water purification plant for 17 days. Typhoon Matsa, following Haitang, hit Taiwan the following year 3–6 August 2005, causing the same problems for 7 days. The torrential rains induced hazards in the reservoir, such as high levels of suspended sediment stopping the water supply for living and industry, and floating timbers in the reservoir that shut off power generation.

The coarse sediment content is transported by bed load; and middle size of sediment moving by suspended load, and the fine contents by wash load to the reservoir (Yu et al. 2000). If these sediments cannot be drained out, then they settle down into the reservoir to form a muddy lake. A major

**Electronic supplementary material** The online version of this article (doi:10.1007/s12665-009-0151-0) contains supplementary material, which is available to authorized users.

C.-Y. Chen
National Chiayi University, No. 300, Syuefu Rd., Chiayi City 60004, Taiwan

L.-K. Chen (✉) · S.-C. Lin · Y.-C. Lin · C.-L. Lee · Y.-T. Wang
National Science and Technology Center for Disaster Reduction (NCDR), 9F., No. 200, Sec. 3, Beisin Rd., Sindian City, Taipei County 23143, Taiwan
e-mail: steven_chen@ncdr.nat.gov.tw

F.-C. Yu
National Chung Hsing University, No. 250, Kuo Kuang Rd., Taichung 402, Taiwan

source of sediment is the landslide-derived sediment yield (Al-Sheriadeh et al. 2000; Korup et al. 2004), and sediment by soil erosion traced using $^{137}$Cs (Stefano et al. 1999; Ambers 2001; Higgitt and Lu 2001; Lu and Higgitt 2001; Walling and Fang 2003; Lee et al. 2005) and by $^{10}$Be and $^{26}$Al (Clapp et al. 2002; Walling et al. 2003) to measure sediment generation and identify sediment sources. Factors that affect the river sediment fluxes for reservoir construction include land clearance and land use change, mining activity, soil and water conservation measures and sediment control programs and climate change (Ambers 2001).

This investigation analyzes the climatic, land use, road building, topologic and geologic conditions and field observation are using GIS to explore the effects attributed to the slopeland hazards and sources leading to the high yield of suspended sediment in the Shihmen reservoir.

## Site location

The Shihmen reservoir is located in Taoyuan County, northern Taiwan. It is adjacent to four counties and close to two townships, namely, Fuxin and Jianshi downstream and upstream, respectively (Fig. 1).

This reservoir, formed out of an earth-embankment dam, is 16.5 km long in a basin area of 763 km$^2$. Thirteen main tributaries flow into the truck Dahan stream. The elevation of the Shihmen reservoir basin is from the southeast for over 3,500 m to the northwest 135 m in the basin. Over 56% of the basin has a gradient over 30°. The effective storage capacity of the reservoir is currently $2.33 \times 10^8$ m$^3$. The average rainfall in the basin area is 2,476 mm/year, and the average water runoff from the reservoir is $1.4 \times 10^9$ m$^3$.

## Historical disasters description

The reservoir operations were shut down during Typhoon Gloria (1963) induced torrential floods, leading to $1.947 \times 10^7$ m$^3$ of suspended sediment accumulated in the reservoir. Two tunnel spillways were constructed in 1979 to drain the suspended sediment at the lower dam of the reservoir. Figure 2 shows the annual silt accumulation in the reservoir. The annual average suspended sediment yield in 2000 was $7.6 \times 10^5$ m$^3$. The sediment production after Typhoon Herb (1996) was $8.67 \times 10^6$ m$^3$. The total suspended sediment yield before Typhoon Aere (2004) was $5.615 \times 10^7$ m$^3$. The increased suspended sediment was about $2.79 \times 10^7$ m$^3$ following Aere. The suspended sediment transport to the reservoir caused by Typhoon Matsa (2005) was about $1 \times 10^7$ m$^3$, and left 69% storage capacity of the reservoir.

Other disasters were flash flood-induced riverbanks incision, landslides, and debris-flows upland of the basin, which brought about 40,000 tons of floating timber after Aere and more than 10,000 tons after Matsa to the lowland of the reservoir (source the Water Resources Agency, http://eng.wra.gov.tw/). The floating timber accumulated in front of the dam and consisted mainly of broken or decayed timber, and bark produced by strong gusts and shallow landslides (Fig. 1, ESM only). The floating timber jammed

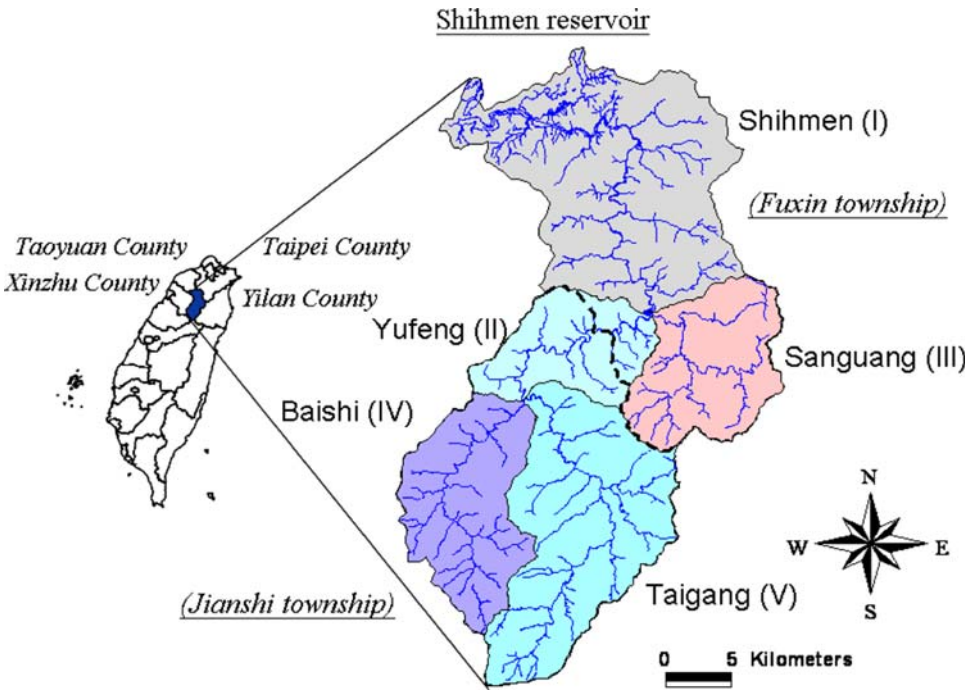


**Fig. 1** Site location of the Shihmen reservoir basin and the drainage network

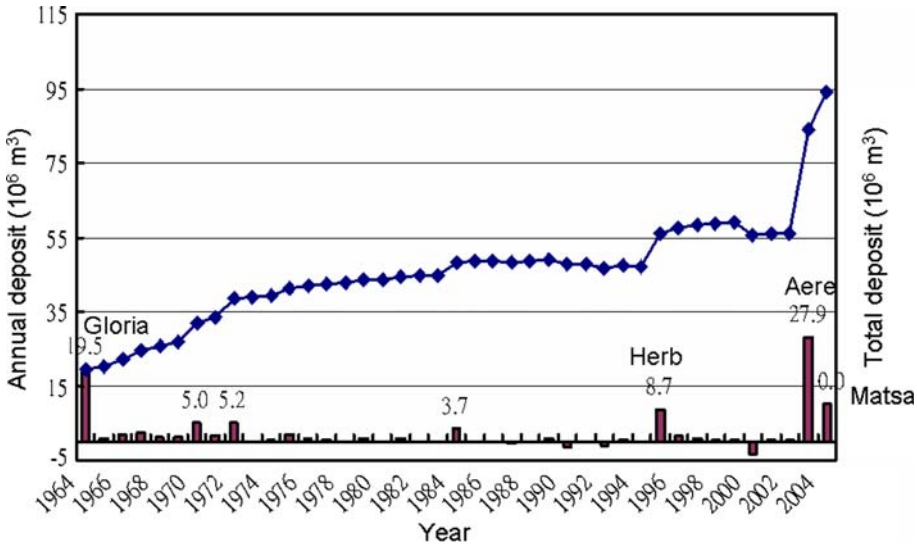


**Fig. 2** Annual suspended sediment yield in the reservoir (source the Water Resources Agency)

the tunnel spillways, and paralyzed the hydropower generation.

The area of naked landslide zone in the Shihmen reservoir basin before 1980 was within 3 km$^2$, and rose to 12.4 km$^2$ owing to Typhoon Herb (1996) (Industrial Technology Research Institute, http://www.itri.org.tw/). The Council of Agriculture (http://eng.coa.gov.tw/) re-investigated the landslide areas following Typhoon Aere (2004), which led to 6.7 km$^2$ of new unvegetated areas in the basin according to aerial photo interpretation. The landslide areas induced by Typhoon Matsa (2005) were 7.0 km$^2$. The maximum landslide was caused by Aere, and its area extended to 0.64 km$^2$ (Council of Agriculture). The differences between the landslides zone induced by Aere and Matsa were small in the sub-catchments of Shihmen (I) and Sanguang (III), but large in Yufeng (II), Baishi (IV) and Taigang (V) sub-catchments (Fig. 1).

Figure 3a illustrates the slopeland disasters upland of the basin for road-related landslide and water-incision-induced riverside landsliding. The aerial photos depict the village isolated by the road-related landslides, and the big landslide at the Baishi catchment (Fig. 3b).

## Analysis of factors contributing to the landslides and suspended sediment yield

The basin was divided into five catchment regions for analysis (Fig. 1). The digital database for the analysis included the digital elevation model (DEM), rainfall records, traffic and river networks, land use and geologic/soil maps. Spatial analysis was performed by ArcGIS 9 (2004) on rainfall distribution, landslides and debris flows, their corresponding soil and geologic conditions, and the impacts of engineering structures (Fig. 4). Aerial photos and field investigations were performed to help identify landslides and debris flows. Field sampling tests were conducted to trace the major sources of suspended sediments.

### Rainfall characteristics analysis

The two typhoons that strongly influenced the basin, Aere (23–26 August 2004) and Matsa (3–6 August 2005) brought more than 1,600 and 1,200 mm of rain, respectively. The two typhoons passed through northern Taiwan, and the rainfall distribution extended from the north to the mountainous regions of middle Taiwan.

Figure 5 displays the distribution of accumulative and maximum rainfall intensity in the basin during Aere (2004) and Matsa (2005). During Aere and Matsa, the maximum accumulative rainfall was 1,607 and 1,274 mm, respectively; the maximum rainfall intensity was 88 and 95 mm/h, respectively. The rains from both these events were concentrated in the Yufeng and Baishi catchments because of the topography and similar paths of the two typhoons. Such a rainfall event historically occurs every 100 years in Baishi, and every 200 years in Yufeng.

### Landslide characteristics analysis

Following Matsa, Fig. 6 depicts the overlaid road network map, the land division map for public or private land, the land reserved for aborigines, gradients of forested land, and the landslide map in the basin. Table 1 summarizes the results of digital themes overlaying and buffer analyses in ArcGIS of landslides induced by Matsa within 40 m of the river channel and roads and their corresponding land divisions in the basin. Typhoon Matsa generated new unvegetated areas of 0.16, 0.15 and 0.11 km$^2$ located mainly in Yufeng, Taigan and Baishi, respectively, for a total of


**Fig. 3** Slopeland hazards at the upland of the watershed for **a** road related landslide (plant bamboo) **b** water incision induced riverside land sliding after Typhoon Matsa (2005) **c** isolated village **d** big land sliding at Baishi catchment for 0.64 km$^2$ after Typhoon Matsa (2005) (aerial photos taken by the Industrial Technology Research Institute)

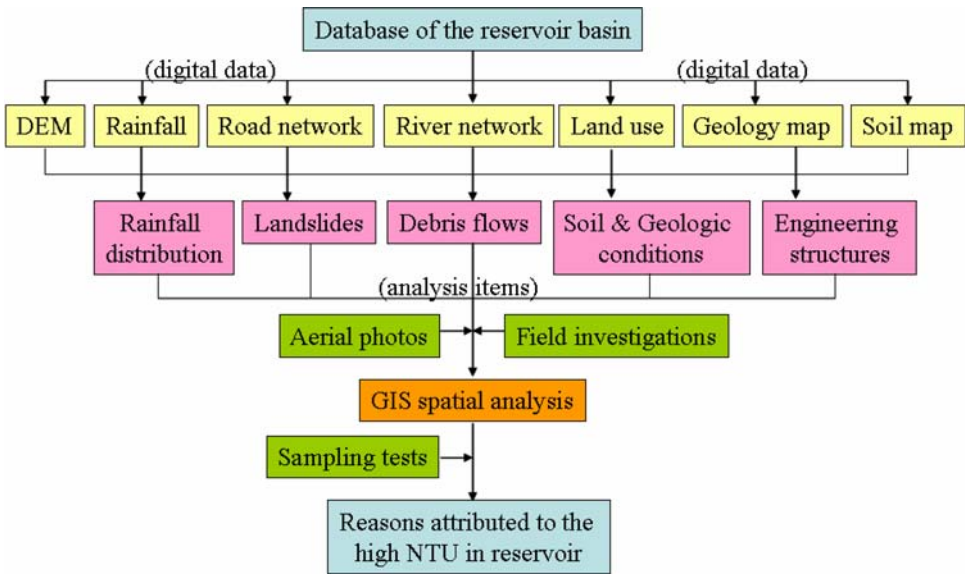


**Fig. 4** Methods of analysis for the contributing factors to the high NTU in reservoir

0.42 km$^2$. The highest landslide ratio (the total landslide areas in the catchment divided by the area of the catchment) was 1.84% in Yufeng, 1.73% in Baishi, and 0.89% in the Taigang catchment.

A digital theme overlay analysis was performed to analyze the landslides and land use in ArcGIS. Of the total landslides, 64.6% (landslide ratio 0.84%) took place in the forested land, 34.7% (landslide ratio 1.38%) in the land reserved for aborigines, and 0.7% (landslide ratio 0.14%) in the public or private land. The landslides were related to topography given that more than 75% occurred in the gradient over 29° (55%). The landslides within a distance of 40 m to the road network and river channel were chosen in GIS spatial analysis; 16.9 and 47.7% of landslides correlated to the road and river networks, respectively. The proportion of landslides related to river channels was highest in Baishi (63.6%), and the proportion of road-related landslides was highest downstream of Yufeng (41.6%, road density 0.0011 km/km$^2$) and high in Shihmen (25.8%, road density 0.0019 km/km$^2$). Catchments with higher road density and human activity had higher landslide ratios.

The landslides were correlated to the rainfall characteristics, topography, land use, river network and roads. Of these factors, the river channels had the strongest effect on

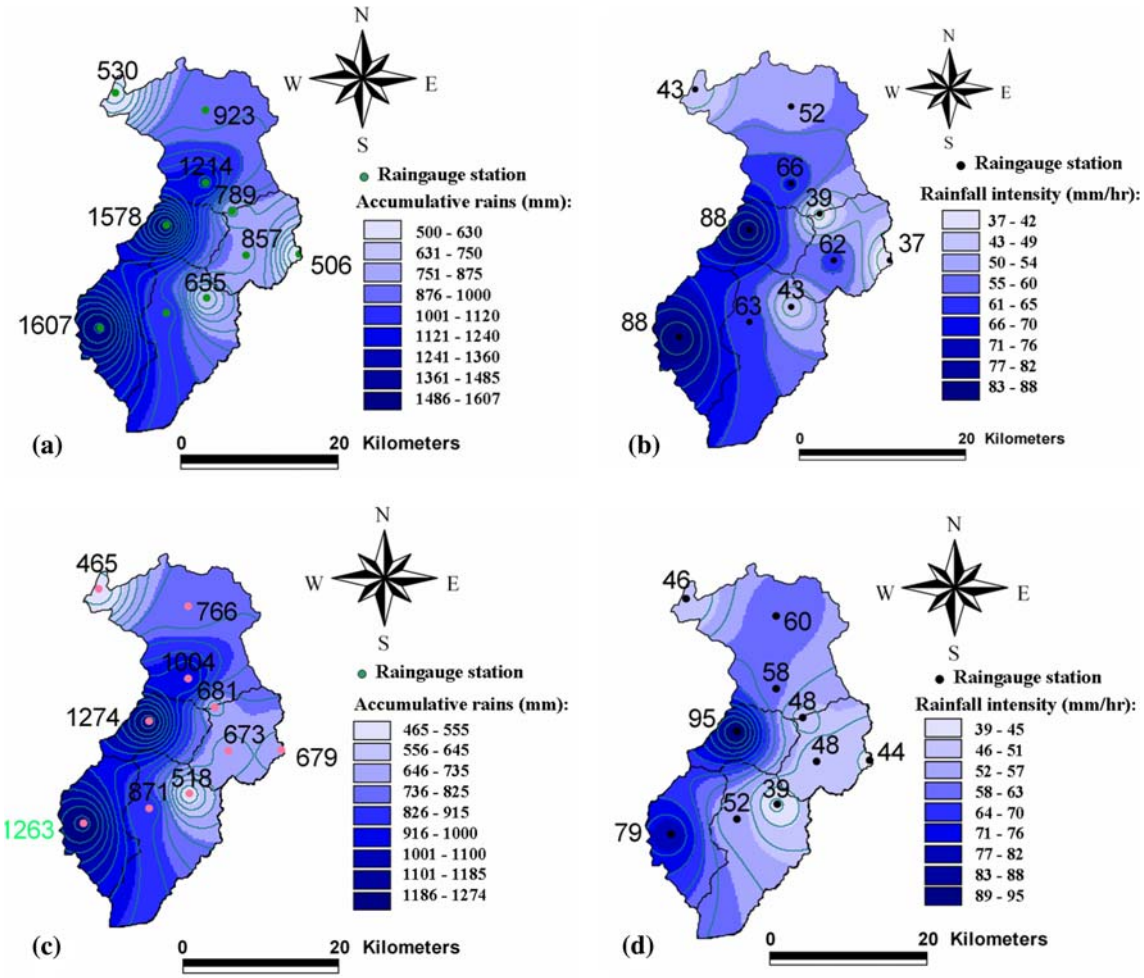


**Fig. 5** Distributed rainfall in the watershed **a** accumulative rainfall and **b** maximum rainfall intensity during Typhoon Aere (from 23 to 26 August 2004) **c** accumulative rainfall and **d** maximum rainfall intensity during Typhoon Matsa (from 3 to 6 August 2005)

landslide activity. River incision, dip slope at riversides, water scouring and landslide pots under the flash flux had a direct impact. Figure 2 (ESM only) illustrates the 200 m river length of the Yufeng catchment, where 67% of landslides, namely, 0.25 $km^2$ within 0.37 $km^2$, related to the river channel initiated at concave pots for scouring by flash flood.

## Debris flow disaster characteristics analysis

The middle and downstream basin has 74 creeks prone to debris inflow (COA 2003). In the aftermath of Aere-induced torrential rains in the watershed, the Central Geologic Survey (http://www.moeacgs.gov.tw/) discovered 76 debris flows in the middle and upstream of the basin, especially as a result of the rains concentrated by the Yufeng, Baishi and Taigang catchments (Fig. 3a, ESM only). Among these, only one debris flow coincided with the two institutes. These debris flows were at steep concaves of valleys, and were initiated by torrential rains.

## Soil and geological conditions

The soil surrounding the reservoir comprises clay, with sandstone/shale stone weathering into yellow to brown and loose red-soil downstream (Fig. 3b, ESM only). The middle stream comprises red soil covered by dark brown or yellow soil, while upstream soils also contain blue lithosols. Table 2 summarizes the sediment contents (classified as CL) in the reservoir, which were 37.6% silt and 60.3% high clay. The gravity was 2.73; the liquid limit was 46.6%, and the plastic index was 22.9%. The clay content of the suspended sediment in the reservoir is the highest among the 17 reservoirs in Taiwan.

The geological structures in the basin are dominated by two faults, four anticlines and two synclines (Fig. 7). The upstream contains argillite, slate, quartzite and coaly shale. Argillite, sandy shale sandstone and slate are located in the middle stream, while sandstone and shale dominate the downstream. In general, the unconfined compressive strength of the rock was 50–100 MPa in the basin, but only

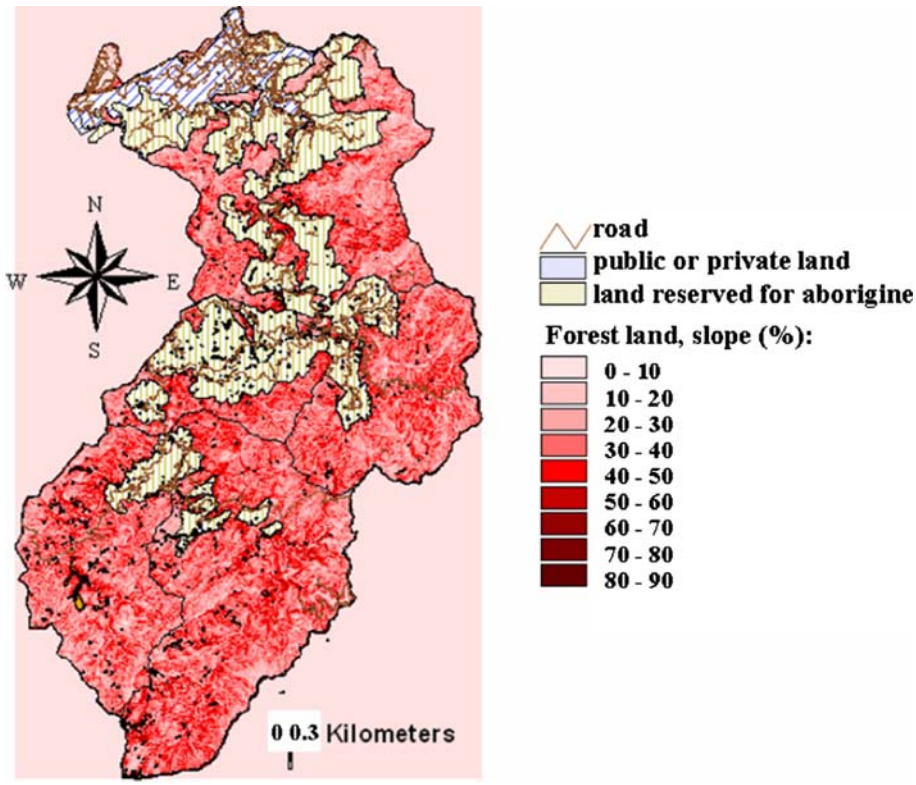


**Fig. 6** Overlaid land use, road, gradient maps and landslides after Typhoon Matsa (2005) in the basin

**Table 1** Typhoon Matsa (2005) induced landslide characteristics analysis

| Catchment | Landslide area ($km^2$) | Landslide ratio[a] (%) | Landslide related to | | |
|---|---|---|---|---|---|
| | | | River Within 40 m (%) | Road | Human activity (%)[b] |
| Shihmen (I) | 1.20 | 0.46 | 54.1 | 25.8 | 56.6 |
| Yufeng (II) | 1.47 | 1.84 | 39.6 | 41.6 | 62.1 |
| Sanguang (III) | 0.51 | 0.48 | 41.2 | 16.0 | 26.6 |
| Baishi (IV) | 2.08 | 1.73 | 63.6 | 5.8 | 7.1 |
| Taigang (V) | 1.77 | 0.89 | 33.5 | 3.7 | 14.9 |
| Total | 7.03 | 0.92 | 47.7 | 16.9 | 30.4 |

[a] The landslide ratio = the landslide areas in the catchment/the catchment area

[b] Including human development, road related and plant land for bamboo

25–50 MPa in the coaly shale layer (Architecture & Building Research Institute, http://www.abri.gov.tw/). Figure 8a and b displays the fragile argillite and the slate, with sandstone interbeds forming joints at riverside. Figure 8c and d displays the orthoclinal slope along the riverside and fault across the stream bed. The gouge in the interbeds is easily washed out by flash flood. The geologic structures and environment form fragile but complex geologic conditions.

Table 3 summarizes the landslides following Matsa and their corresponding geologic strata. The landslide was initiated at the strata of the sandstone and shale. The coaly shale had the highest landslide ratio (1.61%), followed by argillite, shale and phyllite (1.11%), then the strata of argillite, sandy shale sandstone (0.92%).

**Table 2** Sediment content in the reservoir

| AASHTO | Content (%) | | | | Gravity | LL (%) | PI (%) |
|---|---|---|---|---|---|---|---|
| | Gravel | Sand | Silt | Clay | | | |
| CL | 0 | 2.1 | 37.6 | 60.3 | 2.73 | 46.6 | 22.9 |

Source the Architecture & Building Research Institute, http://www.abri.gov.tw

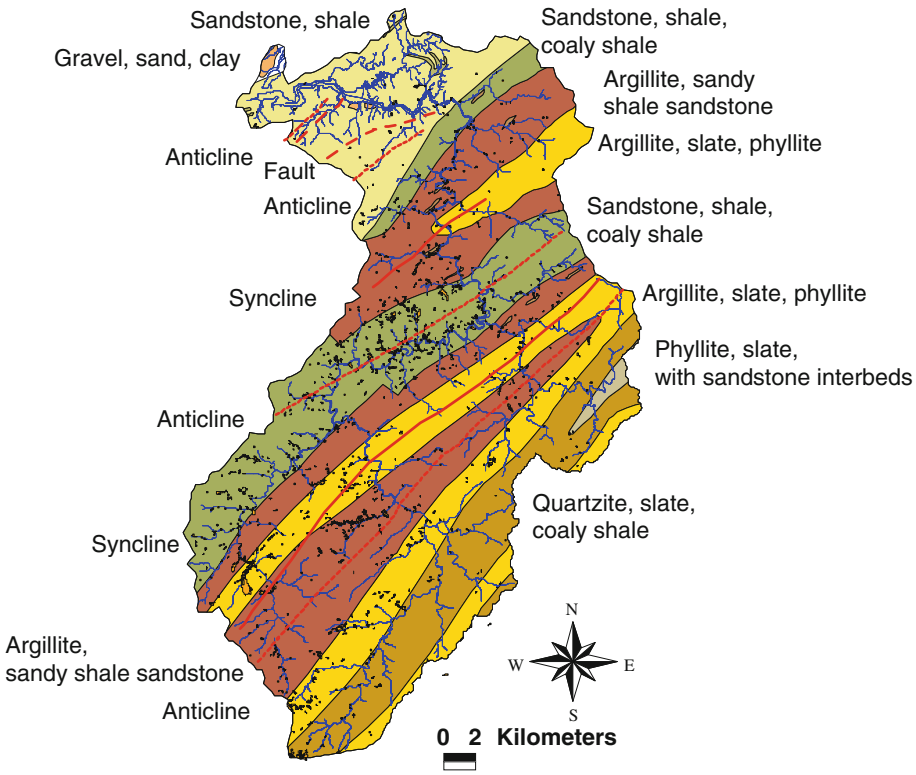


**Fig. 7** Landslides after Typhoon Matsa (2005) and their corresponding geologic conditions in the basin (source Council of Agriculture, Central Geology Survey)

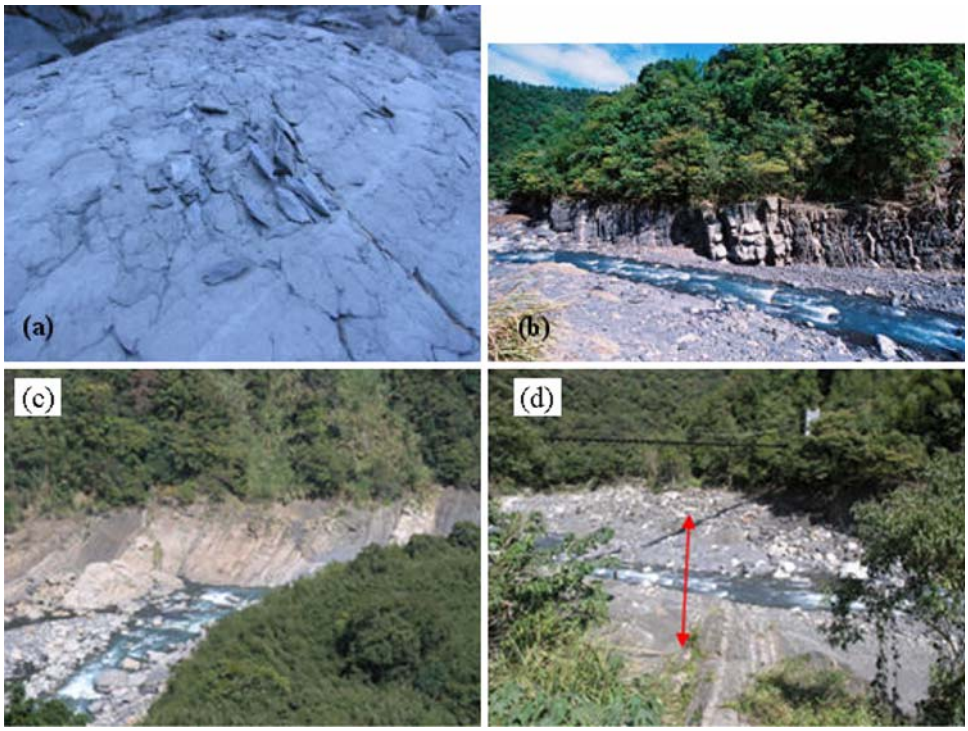


**Fig. 8** Geologic conditions and structures in the basin **a** fragile argillite **b** slate with sandstone interbeds **c** orthoclinal slope at riverside **d** fault across streambed

The impacts of engineering structures on sediment

One hundred twenty-three check dams have been constructed along the tributaries in the basin to allocate and manage the sediment yield from the upland to the lowland since 1965 (Fig. 9). As a result of typhoon events, 38 check dams were damaged, and 74 were full of sediment in 2005. Two large dams in the main river, the Ronghua and Baling

**Table 3** Landslides after Typhoon Matsa (2005) and the corresponding geologic conditions

| Geology | Area in the watershed (%) | Landslide area ($km^2$)/ landslide ratio (%) |
|---|---|---|
| Sandstone, shale, coaly shale | 19.3 | 2.36/1.61 |
| Argillite, sandy shale sandstone | 31.7 | 2.21/0.92 |
| Argillite, slate, phyllite | 22.9 | 1.92/1.11 |
| Phyllite, slate, with sandstone interbeds | 0.6 | 0.002/0.038 |
| Quartzite, slate, coaly shale | 12.3 | 0.36/0.38 |
| Sandstone, shale | 12.6 | 0.17/0.17 |

check dams were covered by debris. The high relief of the check dams caused water to spill, disturbing the settled sediment in the riverbed.

The surrounding soil of the reservoir is composed of clay, with sandstone/shale stone weathering into yellow to brown, and loose red soil downstream (Fig. 3b, ESM only). The middle stream is composed of red soil covered by dark brown or yellow soil; in addition, upstream soils also include blue lithosols. Table 2 summarizes the sediment contents (classified as CL) in the reservoir, for silt 37.6% and high clay fraction for 60.3%, the gravity 2.73, liquid limit 46.6% and plastic index 22.9%. The clay content of the suspended sediment in the reservoir is the highest of the 17 reservoirs in Taiwan.

The geologic structures in the basin are dominated by two faults, four anticlines and two synclines (Fig. 7). In the upstream, argillite, slate, quartzite and coaly shale are distributed. Argillite, sandy shale sandstone, slate is located in the middle stream, and sandstone and shale are dominated in the downstream. In general, the unconfined compressive strength of the rock in the basin is 50–100 MPa, but lower in the coaly shale layer for 25–50 MPa (source the Architecture & Building Research Institute, http://www.abri.gov.tw/). Figure 8a and b shows the fragile argillite and the slate with sandstone interbeds formed joints at riverside. The orthoclinal slope along the riverside and the fault across the streambed are shown in Fig. 8c and d. The gouge in the interbeds is easily washed out by flash flood. The geologic structures and environment form fragile but complicated geologic conditions.

Table 3 summarizes the landslides following Matsa and their corresponding geologic strata. The landslide began at the strata of sandstone, shale; coaly shale has the highest landslide ratio (1.61%), and then argillite, shale, phyllite (1.11%), and third is at the strata of argillite, sandy shale sandstone (0.92%).

## Sampling tests

Figure 4 (ESM only) displays the confluence of lower suspended sediment from the Sanguang stream, and the higher suspended sediment from Yufeng stream to the truck of Tahan stream. Field observation results demonstrate that the road-related landslides had yellow soil. The water in the middle stream was also yellow, but the water upstream and lower reach of the reservoir was gray to black. These findings demonstrate that the suspended sediments are linked to the geologic conditions and types of weathered soil mantle. Additionally, the major suspended sediments were sourced from the higher landslide density of the trunk riversides.

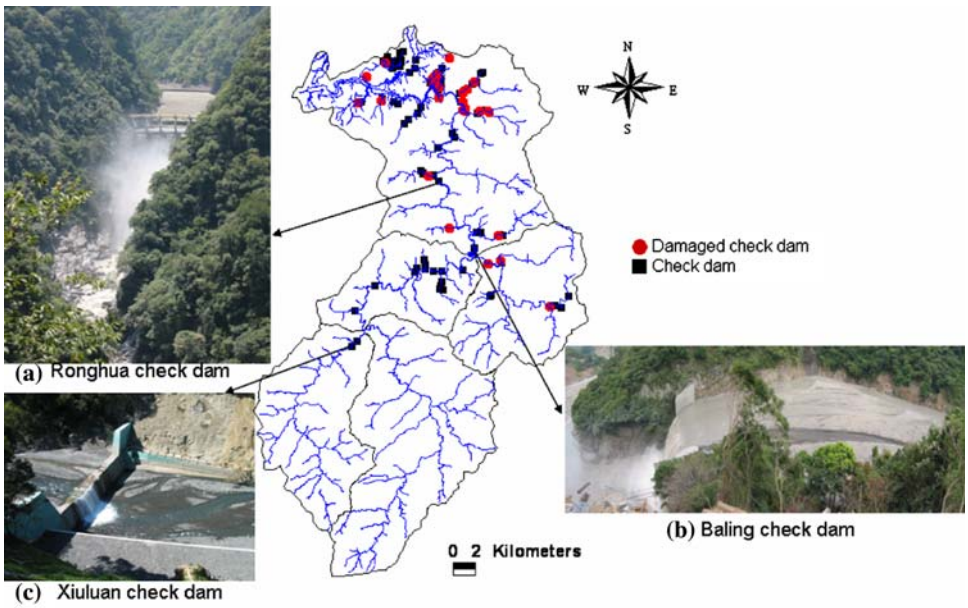


**Fig. 9** Site location of the check dams in the watershed

**Table 4** Site location of the sampling tests

| No. | Location (2005/08/23) | No. | Location (2005/09/06) | NTU |
|---|---|---|---|---|
| 1–1 | Upstream of Baishi creek | 2–1 | Landslide site | - |
| 1–2 | Confluence | 2–2 | Forest land | |
| 1–3 | Landslide site | 2–3 | Forest land | |
| 1–4 | Xiuluan check dam | 2–4 | Upstream of landslide site | |
| | | 2–5 | Downstream of landslide site | |
| | | 2–6 | Downstream of Xiuluan check dam | + |

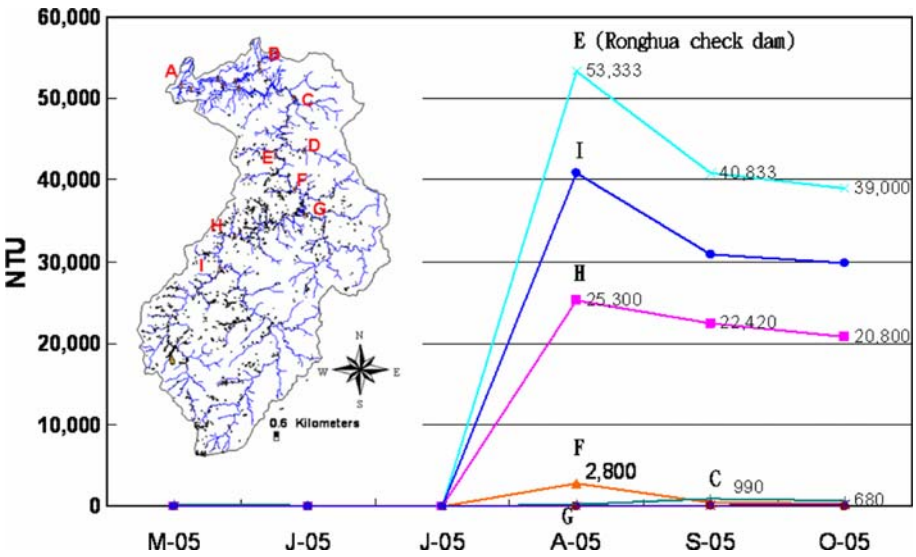


**Fig. 10** Recorded NTU at monitoring stations from March to October 2005 (source the Northern Region Water Resources Office)

To explore the sources of suspended sediment yield, the Council of Agriculture undertook two water quality sampling tests at the Baishi catchment (Fig. 5, ESM only). The sampling test on 23 August 2005 was located near the side of the large landslide in Baishi (0.64 $km^2$), and the sampling test undertaken on 6 September 2005 was located between the Xiuluan check dam and the Baishi large landslide site (Table 4).

The highest peak discharge of the Shihmen reservoir watershed in history was 10,141 $m^3/s$ in 1963 during Typhoon Gloria. The peak discharge of Aere in 2004 was 8,594 $m^3/s$ over 40 h, occurring in the basin. Matsa generated a peak discharge of 5,322 $m^3/s$ for a rainfall duration of 24 h. The torrential rain-induced flash flood raised the transportation of suspended sediment from upland to downstream, and scoured debris masses in the riverbed, owing to sediment yield controlled mainly by flood magnitude and frequency (Ambers 2001). Figure 10 illustrates the water quality measurements recorded by the nine monitoring stations following Matsa. The monitoring station at the Ronghua check dam had the highest concentration up to 53,333 NTU, followed by the two stations in the Yufeng catchment. The sediment concentration rose from 13.1 to 15.6, its original value, from 2002 to 2006 during the typhoon events in the Yufeng catchment (Chu and Hsu 2007). The high relief of check dams is thought to have stirred the riverbed sediment, and the fine silt content would take approximately 2 days to re-settle. Typhoon Aere generated 250,000 NTU at the reservoir outlet for water supply (E.L. 195 m) lasting 45 days, and Matsa produced 46,000 NTU under a water depth of 45 m lasting 25 days down to the general standard 1,000 NTU (Northern Region Water Resources Office).

## Conclusions

In summary, results of field observations and sampling tests demonstrate that suspended sediment begins from the Xiuluan check dam, and that landslides do not necessarily induce long-term high NTU at the landslide location. The suspended sediment is speculated to be higher at the

Yufeng catchment corresponding to the strata of sandstone, shale and coaly shale. The inferred sediment content was about 3,000–10,000 NTU, and was caused by Matsa-induced landslide-derived sediment. Additionally, soil erosion and previously deposited debris masses in the riverbed contributed to the sediment yield in the reservoir. This finding is confirmed by the tracing analysis of $^{137}$Cs by Lee et al. (2005), who found that landslide-derived sediment occurred primarily upstream or confined valley, and declined in volume with proximity to the reservoir.

Slopeland-related disasters in the basin include debris flows in the gully, hill slope landslides, seepage-induced soil erosion and road-related landslides. The high suspended sediment yield has interrupted reservoir operation. The slopeland disasters in the basin have been attributed to torrential rains, steep topographic characteristics, road construction, land use changes, community development in the mountain areas, river incision and complex geologic structures and conditions. Numerous factors have contributed to the high suspended sediment yield in the reservoir, including high torrential rains inducing flash flooding, steep topographic properties and landslide derived and artificial activities. The erodable geologic conditions and long-term debris deposited in riverbeds play a significant role in the sediment yields. The AGNPS (Young et al. 1987) model predicted an average basin sedimentation depth of about 2.5 mm/year, which exceeds the depths observed in the US (Lo 1994). Although the landslide ratio (0.9%) of the basin is lower than that of other reservoirs in Taiwan, the disasters induced by high suspend sediment have raised the issues of soil and water conservation in the upland and the importance of management (Chen et al. 2007) and operation for the reservoir (Chang and Chang 2001; Hsu and Wei 2007; Chang 2008). Those landslides will jeopardize the design capacity of the reservoir if they are not controlled (Al-Sheriadeh et al. 2000).

**Acknowledgments** The authors appreciated the Water Resources Agency, Central Weather Bureau, Central Geology Survey, Soil and Water Conservation Bureau, Industrial Technology Research Institute, Architecture and Building Research Institute for providing valuable materials for this study. The constructive suggestions of the anonymous reviewers are appreciated.

## References

Al-Sheriadeh MS, Malkawi AIH, Al-Hamdan A, Abderahman NS (2000) Evaluating sediment yield at King Talal Reservoir from landslides along Irbid-Amman Highway. Eng Geol 56:361–372

Ambers RKR (2001) Using the sediment record in a western Oregon flood-control reservoir to assess the influence of storm history and logging on sediment yield. J Hydrol 244:181–200

ArcGIS 9 (2004) Introduction to ArcGIS 9 parts I & II. New York Street, Redlands, CA, USA. Environment System and Research Institute

Chang LC (2008) Guiding rational reservoir flood operation using penalty-type genetic algorithm. J Hydrol 354:65–74

Chang LC, Chang FJ (2001) Intelligent control for modelling of real-time reservoir operation. Hydrol Process 15:1621–1634

Chen SC, Lai YC, Wang CL (2007) Evaluation model for watershed sediment management of the Shihmen reservoir in Taiwan. Geophys Res Abstr 9:08593

Chu YT, Hsu ML (2007) The relationship between discharge and suspended sediment concentration at typhoon events in Yu-Feng catchment. J Geogr Sci 49:1–22

Clapp EM, Bierman PR, Caffee M (2002) Using $^{10}$Be and $^{26}$Al to determine sediment generation rates and identify sediment source areas in an arid region drainage basin. Geomorphology 45:89–104

COA (2003) The map of hazardous debris-flow streams in Taiwan, scale: 1/250,000, Council of Agriculture, Republic of China (in Chinese)

Higgitt DL, Lu XX (2001) Sediment delivery to the three gorges: I. Catchment controls. Geomorphology 41:143–156

Hsu NS, Wei CC (2007) A multipurpose reservoir real-time operation model for flood control during typhoon invasion. J Hydrol 336:282–293

Korup O, McSaveney MJ, Davies RH (2004) Sediment generation and delivery from large historic landslides in the Southern Alps, New Zealand. Geomorphology 61:189–207

Lee HY, Borghuis AM, Chiu YJ (2005) Estimation of soil erosion in the reservoir watersheds using isotope $^{137}$Cs. Taiwan-Russia Bilateral Symposium on water and Environmental Technology, Taipei, Taiwan, pp 33–49

Lo KFA (1994) Quantifying soil erosion for the Shihmen reservoir watershed, Taiwan. Agric Syst 45:105–116

Lu XX, Higgitt DL (2001) Sediment delivery to the three gorges II: local response. Geomorphology 41:157–169

Stefano CD, Ferro V, Porto P (1999) Linking sediment yield and Caesium-137 spatial distribution at basin scale. J Agric Eng Res 74:41–62

Walling DE, Fang D (2003) Recent trends in the suspended sediment loads of the world's rivers. Glob Planet Change 39:111–126

Walling DE, He Q, Whelan PA (2003) Using $^{137}$Cs measurements to validate the application of the AGNPS and ANSWERS erosion and sediment yield models in two small Devon catchments. Soil Tillage Res 69:27–43

Young RA, Onstand CA, Bosch DD, Anderson WP (1987) AGNPS: agricultural non-point source pollution model. A watershed analysis tool. USDA Conservation Research Report, vol 35, pp 86

Yu WS, Lee HY, Hsu SM (2000) Experimental study on the deposition behavior of fine sediment in a reservoir. J Hydraul Eng 126(12):912–920